Fermi National Accelerator Laboratory

FERMILAB-Pub-92/156

A Search for Solar Axions

F.A. Nezrick

Fermi National Accelerator Laboratory
P.O. Box 500, Batavia, Illinois 60510

D.M. Lazarus and G.C. Smith

Brookhaven National Laboratory
Upton, New York 11973

R. Cameron, A.C. Melissinos, G. Ruoso, and Y.K. Semertzidis

University of Rochester
Rochester, New York 14627

June 1992

Submitted to *Physical Review Letters*

Operated by Universities Research Association Inc. under Contract No. DE-AC02-76CHO3000 with the United States Department of Energy

A SEARCH FOR SOLAR AXIONS

D.M. Lazarus and G.C. Smith

Brookhaven National Laboratory, Upton, NY 11973

R. Cameron,[a] A.C. Melissinos, G. Ruoso,[b] and Y.K. Semertzidis[c]

Dept. of Physics and Astronomy

University of Rochester, Rochester, NY 14627

F.A. Nezrick

Fermi National Accelerator Laboratory

P.O. Box 500, Batavia, IL 60510

We have searched for a flux of axions produced in the sun by exploiting their conversion to x-rays in a static magnetic field. The signature of a solar axion flux would be an increase in the rate of x-rays detected in a magnetic telescope when the sun passes within its acceptance. From the absence of such a signal we set a 3σ limit on the axion coupling to two photons $g_{a\gamma\gamma} = (1/M) < 3.9 \times 10^{-9}$ GeV^{-1}, provided the axion mass $m_a < 0.11$ eV.

PACS numbers: 18.80.Am, 18.80.Gt

Current theories of the elementary particles predict the existence of low mass scalar or pseudoscalar particles. These arise naturally when a global symmetry is spontaneously broken and are referred to as Nambu-Goldstone bosons [1]. Of such particles, one that has received much attention is the axion, which emerges when the Peccei-Quinn symmetry is broken [2]. It was originally thought that the P-Q symmetry breaking, which was introduced to explain the absence of CP violating effects in strong interactions, occurs at the energy scale of the weak interactions, $f_a \sim 250$ GeV. The existence of axions in this region has been experimentally excluded [3].

It is now believed [4] that the symmetry breaking that gives rise to the axion occurs at much higher energies, in the range of $10^8 - 10^{13}$ GeV. The mass, m_a, of the axion is related to the symmetry breaking scale f_a through

$$m_a f_a = \frac{N\sqrt{z}}{1+z} m_\pi f_\pi \sim 3.7 \times 10^{-2}\ \mathrm{GeV}^2 \tag{1}$$

with $z = m_u/m_d \simeq 0.56$, m_π being the mass of the π^0 and f_π the pion decay constant. The axion couples to two photons through a triangle anomaly, and the coupling can be expressed as

$$g_{a\gamma\gamma} = \frac{\alpha}{2\pi}\frac{N}{f_a}(E/N - 1.95) \equiv \frac{1}{M} \tag{2}$$

Here E and N are respectively the color and electromagnetic anomalies of the Peccei-Quinn symmetry and $\alpha = 1/137$ is the fine structure constant [4].

Axions that couple directly to electrons through an *eea* vertex provide a very efficient energy loss mechanism and their relative coupling is excluded by many orders of magnitude by the cooling rates of the sun, the red giants and the supernova SN1987A [4,5]. However, "hadronic axions", which do not directly couple to leptons, interact with matter primarily through a two photon vertex [6]. They can still be produced in the solar interior, provided the axion luminosity is less than the corresponding photon luminosity so as to not conflict with the apparent age of the sun. Such axions, if they exist, must be produced abundantly in the interior of the sun through the Primakoff effect as indicated in Fig. 1a, the rate being proportional to M^{-2}. Figure 1b shows the inverse process by which axions are converted to photons in the presence of an external field.

The spectrum of the axions emitted by the sun has been published [7] and is shown in Fig. 2a where the rate refers to the axion flux at the surface of the earth. Since axions are produced by blackbody radiation at the center of the sun, their energy is typically in the few keV range. The total axion luminosity is

$$L_a = 1.7 \times 10^{-3} L_{\odot} \left(\frac{10^{10}\mathrm{GeV}}{M}\right)^2 \text{Watts} \tag{3}$$

where $L_{\odot} = 3.8 \times 10^{26}$ Watts is the photon luminosity of the sun and the integrated axion luminosity in our range of sensitivity, $2.8 - 8.8$ keV, is

$$L_{int} = 2.5 \times 10^{15} \left(\frac{10^{8}\mathrm{GeV}}{M}\right)^2 (\mathrm{cm}^2 - \mathrm{sec})^{-1} \tag{4}$$

Solar axions can be detected by the inverse process, namely by their reconversion into x-rays in the presence of a magnetic field transverse to their direction of propagation [8]. The conversion process is coherent when the axion and photon fields remain in phase over the length of the magnetic field region [9]; in that case the conversion probability is given by

$$P_{\gamma} = 3.9 \times 10^{-16} \left[\frac{L}{180\mathrm{cm}}\right]^2 \left[\frac{B}{2.2\mathrm{T}}\right]^2 \left[\frac{10^{8}\mathrm{GeV}}{M}\right]^2 \tag{5}$$

where L is the length of the magnetic field and B its strength. In this experiment $L = 180$ cm and $B = 2.2$ T.

The coherence condition requires

$$\Delta\phi = L\Delta k = \frac{1}{2} L\omega \left(\frac{m_a}{\omega}\right)^2 < \pi \tag{6}$$

For our detector ($L = 180$ cm, $\omega \sim 3$ keV) the inequality (6) is satisfied for $m_a < 0.05$ eV. However, coherence can be maintained for higher masses if the conversion region is filled with a low Z gas such as helium. Because of the negative dispersion of x-rays the phase velocity of the x-ray field is reduced according to [10]

$$k = \omega(1 - \omega_p^2/2\omega^2) \tag{7}$$

where $\omega_p^2 = 4\pi n_e r_0 c^2$ is the plasma frequency. For helium gas at 1 atmosphere, $\omega_p = 4.1 \times 10^{14}$ rad/s ~ 0.3 eV.

The axion converter consisted of a six-inch diameter vacuum pipe placed in the gap of an iron core dipole magnet with aperture of 18 inches horizontal by 6 inches high and 72 inches long [11] which was oriented so that its long axis pointed along the azimuth of the setting sun. This provided a time window of approximately 15 minutes every day during which the line of sight through the vacuum region pointed directly to the sun. Attached to the end of the evacuated pipe opposite the sun was an x-ray proportional chamber [12] with a 2×10 cm^2 window. The window which was 0.0005 inch thick mylar, served as one of the cathodes. The proportional chamber was operated with a P10 (Argon with 10% Methane) gas mixture at one atmosphere.

The proportional chamber was calibrated with an ^{55}Fe source which emits a monochromatic x-ray line of energy E = 5.9 keV. With no differential pressure on the thin window, the anode pulse height resolution at 6 keV corresponds to a FWHM = 20%. However, when one side of the window was at vacuum, the window was slightly deformed and the peak became significantly broader. The 5.9 keV line is shown in Fig. 2b under this condition. We have convolved the axion spectrum of Fig. 2a with the energy loss in the window and the effects of resolution to obtain the expected x-ray spectrum from axion conversions in our detector. This is displayed in Fig. 2c.

The detector signals were collected by a charge sensitive preamplifier, followed by a shaping amplifier whose output was analyzed by a LeCroy 2259B CAMAC ADC. Data was acquired through an IBM/PC 386 computer which recorded the pulse height from the proportional chamber and the time of arrival. The data was analyzed on-line and also written to disk. The background spectrum is shown in Fig. 3a; the dashed curve in Fig. 3a indicates the expected spectrum if the rate of converted axions equaled the background rate. Events were selected between channels 250 and 850; this corresponds to $2.8 < E_\gamma < 8.8$ keV and is a reasonable match to the bulk of the expected axion spectrum (cf. Fig.

2c). The background rate R_γ for these selected events was approximately 2 Hz.

Data were taken for about two hours centered around sunset on January 25 and 26, 1992 with the pipe evacuated; this covers the mass range $m_a < 0.05$ eV. Further data were taken on January 27 and 28 with helium gas in the magnetic volume, at pressures of 55 and 100 torr respectively thereby extending the range of sensitivity to masses as large as 0.11 eV. The rate of events within the $2.8 < E_\gamma < 8.8$ keV energy range are plotted as a function of time in Fig. 3b; the rate has been calculated for 30 second time intervals and the figure refers to the vacuum data. No peak is seen at the time of sunset when the sun moved across the detector acceptance. The dashed curve shows the expected signal if the peak solar axion rate was $R_\gamma = 2$ Hz; it is a Gaussian with standard deviation $\sigma_t = 500$ seconds and closely approximates the acceptance of the detector as a function of time for the dates when the data was taken.

All three data sets were searched for an increased x-ray rate at sunset by fitting the data to a function

$$R = R_0 + R_0' t + R_\gamma exp[-(t_0 - t)^2/2\sigma_t^2] \tag{8}$$

where t_0 is the sunset time and $\sigma_t = 500$ s. The solid line in Fig. 3b is the result of the fit to the vacuum data. The R_0' term was less than 1.4×10^{-5} for all three fits, reflecting the stability of the system against counting rate drift. To extract the limits on M, we employ the spectrum of Fig. 2a properly normalized to include detector efficiency which accounts for losses in the spectrum due to x-ray absorbtion in the mylar window separating the proportional chamber from the vacuum pipe and production of photoelectrons in the detector gas. The weighted average efficiency over our region of spectral sensitivity was $\epsilon = 0.4$.

Table I summarizes the fits including the rates R_γ and the corresponding lower limits on M at the 3σ level. We then conclude:

$$M > 2.55 \times 10^8 \text{ GeV}(99.7\%\text{C.L.}) \qquad \text{for } m_a < 0.11 \text{ eV}$$

Our results do not reach the sensitivity required to determine the presence of hadronic axions since the coherence condition of Eqs. (6) and (7) limits the axion mass range accessible to 0.11 eV while hadronic and DFSZ[13] axion couplings lead to the diagonal lines indicated by "axion models" in Fig. 4. The result reported here should then be considered to apply more generally to Nambu-Goldstone bosons satisfying the requirements of solar Primakoff production and coherent conversion in our detector.

Although this result was obtained in a laboratory experiment, it depends on the solar model for the prediction of the expected spectrum. The limit on M is at the level expected from considerations of the solar luminosity and thus its cooling rate (see Eq.(3)). However, it is an improvement of nearly two orders of magnitude over the limits that have been placed on M by purely terrestrial experiments [14]. It is clear that modifications of this apparatus to track the sun during a larger fraction of the day and using a higher field and longer magnet can improve the limit on M by another order of magnitude [15].

To place this result in context we show in Fig. 4 the limits on the axion coupling to two photons, $g_{a\gamma\gamma}$, as a function of axion mass obtained by other experiments: laser experiments [12], microwave cavity experiments [16], telescope search [17] and particle decay experiments [3]. We also show the limits deduced from the luminosity of the sun, of the red giants and of SN1987A [4,5]. The heavy line is the relation between m_a and $g_{a\gamma\gamma}$ implied by Eqs. (1,2); this presumes that the coupling parameter $\zeta = (E/N - 1.95) = (8/3 - 1.95) = 0.72$ (see Ref. [4] for more details). We again note that for these axion models $M > 2.55 \times 10^8$ GeV corresponds to a mass $m_a < 20$ eV. Our result has excluded a significant fraction of this space but has inadaquate sensitivity to reach the line corresponding to the axion models. However as the sensitivity of the solar experiment improves, the detection window will encompass the predicted region of the hadronic axion.

We thank Brookhaven National Laboratory for its continuing support of this research program and in particular Dave Dayton and Al Pendzick for their invaluable help in setting up the experiment. This work was supported in part by the U.S. Dept. of Energy under contracts DE-AC02-76ER13065, DE-AC02-76CH00016, and DE-AC02-76CH03000.

[(a)] Present address: Department of Physics, University of Western Ontario, London, ON N6A 3K7, Canada

[(b)] Present Address:Dipartimento di Fisica "Galileo Galilei" dell' Università di Padova, I-35100 Padova, Italy

[(c)] Present address: Physics Department, Brookhaven National Laboratory, Upton, NY 11973

References

[1] Y. Nambu, Phys. Rev. Lett. **4**, 380 (1960); J. Goldstone, Nuovo Cimento **19**, 154 (1961).

[2] R.D. Peccei and H.R. Quinn, Phys. Rev. Lett. **38**, 1440 (1977); Phys. Rev. **D16**, 1791 (1977); S. Weinberg, Phys. Rev. Lett. **40**, 223 (1978). F. Wilczek, Phys. Rev. Lett. **40**, 279 (1978).

[3] W.T. Ford *et al.*,, Phys. Rev. **D33**, 3472 (1986); H.J. Behrend *et al.*, Phys. Lett. **B176**, 247 (1986). C. Hearty *et al.*, Phys. Rev. Lett. **58**, 1711 (1987); U. Amaldi, G. Carboni, B. Jonson, and J. Thun, Phys. Lett. **B153**, 444 (1985), searched for $\gamma+$ nothing in the decays of orthopositronium; however, they are not sensitive to pseudoscalars of mass < 100 keV; A. Bross *et al.*, Phys. Rev. Lett. **67**, 2942 (1991); M.S. Alam *et al.*, Phys. Rev. **D27**, 1665 (1983); N.J. Baker *et al.*, Phys. Rev. Lett. **59**, 2832 (1987).

[4] M.S. Turner, Physics Reports **197**, 67 (1990).

[5] C. Raffelt, Physics Reports **198**, 1 (1990).

[6] J.E. Kim, Phys. Rev. Lett. **43**, 103 (1979); M.A. Shifman *et al.*, Nucl. Phys. **166**, 493 (1980).

[7] K. Van Bibber *et al.*, Phys. Rev. **D39**, 2089 (1989); G. Raffelt, Phys. Rev. **D33**, 897 (1986).

[8] P. Sikivie, Phys. Rev. Lett. **51**, 1415 (1983); Phys. Rev. Lett. **61**, 783 (1988).

[9] G. Raffelt and L. Stodolsky, Phys. Rev. **D37**, 1237 (1988).

[10] J.D. Jackson, "Classical Electrodynamics", p. 315, second edition, John Wiley and sons ed., 1975.

[11] G.T. Danby, AGS Internal Report, GTD-2, Dec 26 (1961).

[12] G.C. Smith, Nuclear Instruments and Methods **222**, 230 (1984).

[13] M. Dine, W. Fischler and M. Srednicki, Phys. Lett. **104B**, 199 (1981); A. R. Zhitnitsky, Sov. J. Nucl. Phys. **31**, 260 (1980).

[14] Y. Semertzidis *et al.*, Phys. Rev. Lett. **64**, 2988 (1990); G. Ruoso *et al.*, University of Rochester Report No. UR-1248 (to be published).

[15] Such an experiment is in progress at the Institute for Nuclear Physics, Novosibirsk. P. Vorobyov (private communication).

[16] S. DePanfilis *et al.*, Phys.Rev. Lett. **59**, 839 (1987); W.U. Wuensch *et al.*, Phys. Rev. **D40**, 3153 (1989), C. Hagmann *et al.*, Phys. Rev. **D42**, 1297 (1990).

[17] M. Bershady, M. T. Ressel and M.S. Turner, Phys. Rev. Lett. **66**, 1398 (1991).

Figure Captions

Fig 1 (a) Axion production by the Primakoff effect. (b) Axion conversion to a photon by the same process.

Fig 2 (a) The calculated differential spectrum of axions reaching the surface of the earth for $M = 10^9$ GeV (from ref. 5). (b) Pulse height spectrum of the 5.9 keV Fe^{55} line under the operating (distorted window) conditions of the detector. (c) The pulse height spectrum for converted solar axions when the spectrum in (a) of the figure is corrected for window absorption and convolved with the experimental resolution.

Fig 3 (a) The background spectrum in the detector. The dashed curve shows the expected shape if the converted axion rate equals the background rate. (b) The event rate for $2.8 < E_\gamma < 8.8$ keV plotted as a function of time every 30 seconds for the vacuum data. The dashed curve shows the expected solar axion signal if that rate reaches a peak value of 2 Hz. The solid line is a best fit to the data and shows no enhancement at the sunset time.

Fig. 4 The limits on Nambu-Goldstone coupling to two photons vs. the boson mass from several experiments. Also shown are the astrophysical limits. The solid line labeled axion models encompasses the predictions of the "hadronic" [6] and DFSZ [13] axion models.

TABLE I. Axion mass ranges, fit parameters, and 3σ level limits on M for the three He pressures used in the experiment.

Pressure(Torr)	m_a(eV)	R_0(Hz)	R_γ(Hz)	$\chi^2/d.o.f.$	M(GeV)(3σ limit)
0	< 0.050	2.127 ± 0.037	-0.036 ± 0.055	0.67	2.79×10^8
55	$0.050 - 0.086$	2.087 ± 0.055	-0.037 ± 0.074	1.11	2.55×10^8
100	$0.086 - 0.110$	1.970 ± 0.034	-0.073 ± 0.060	1.10	2.92×10^8

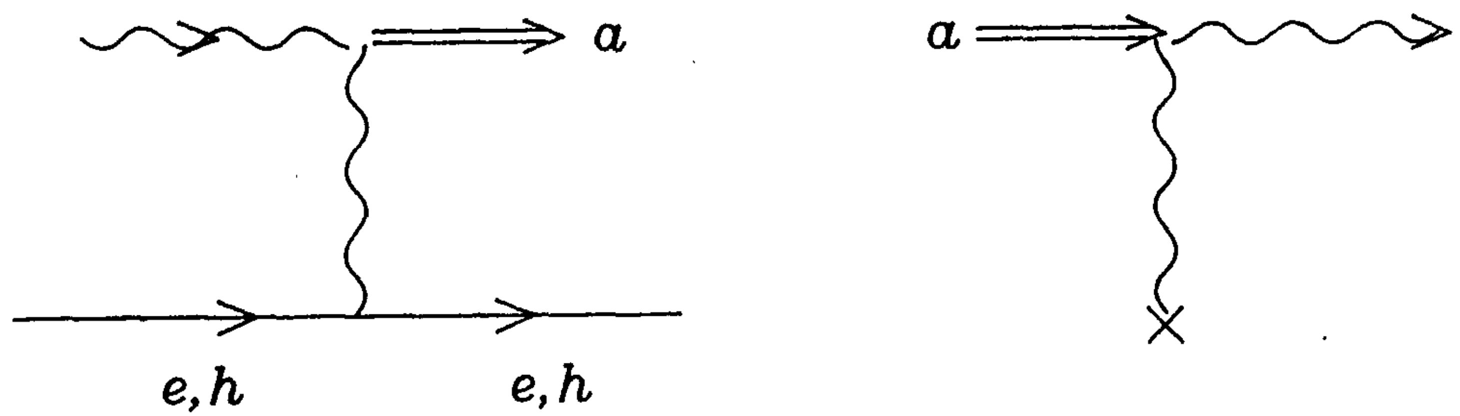

(a) (b)

Figure 1

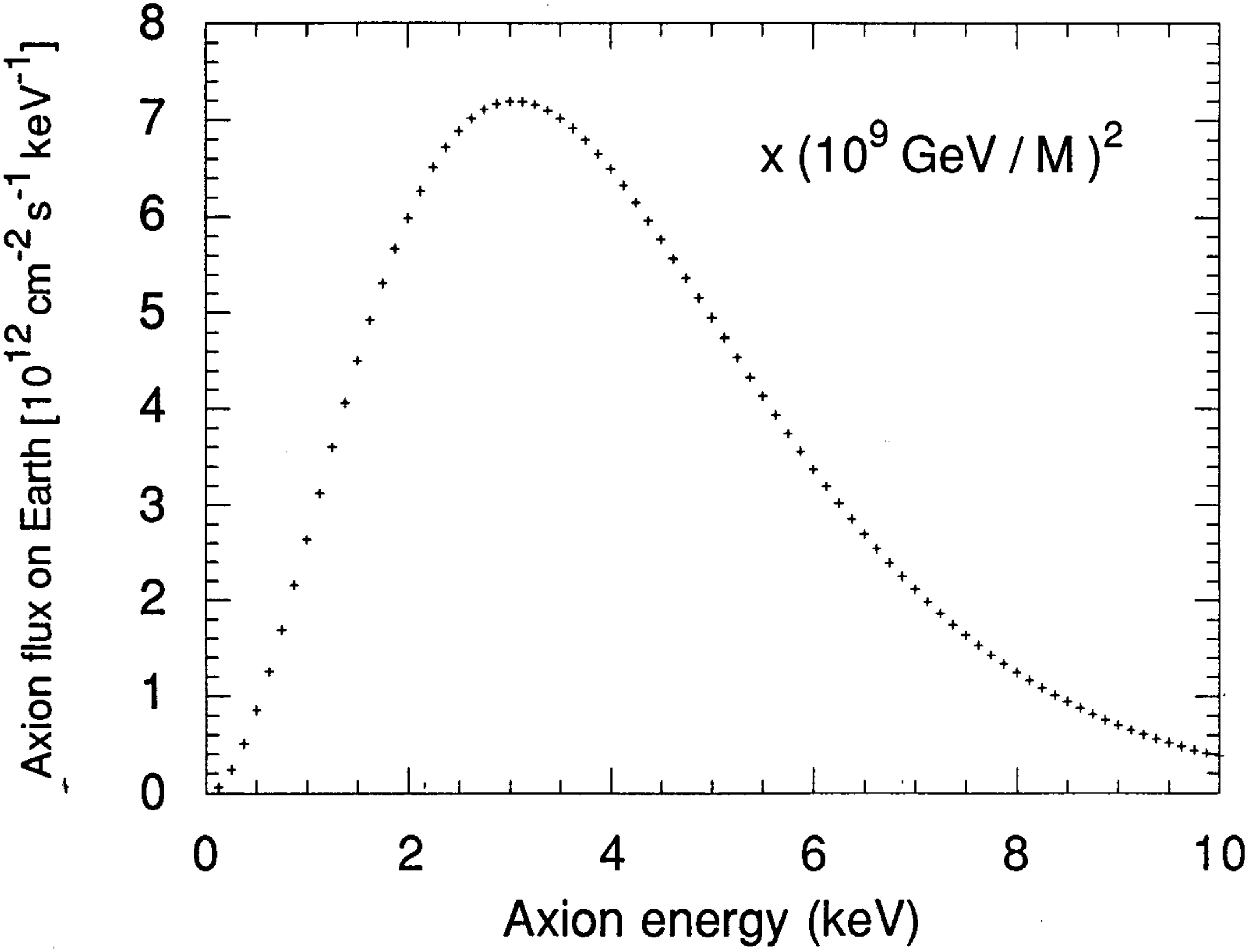

Axion flux on Earth [10^{12} cm^{-2} s^{-1} keV^{-1}]
x (10^9 GeV / M)^2
Axion energy (keV)
0
1
2
3
4
5
6
7
8
0
2
4
6
8
10

Figure 2a

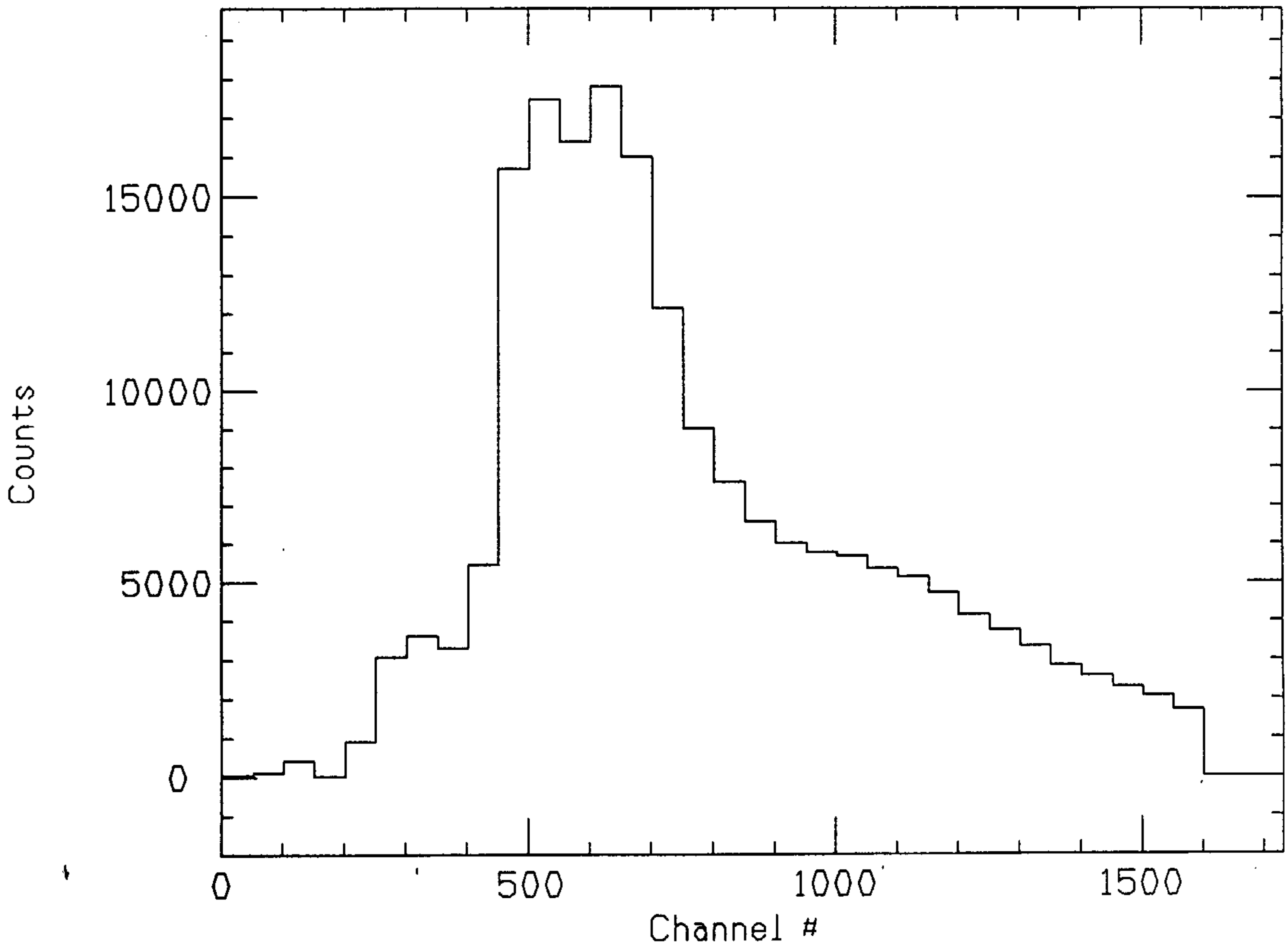

Figure 2b

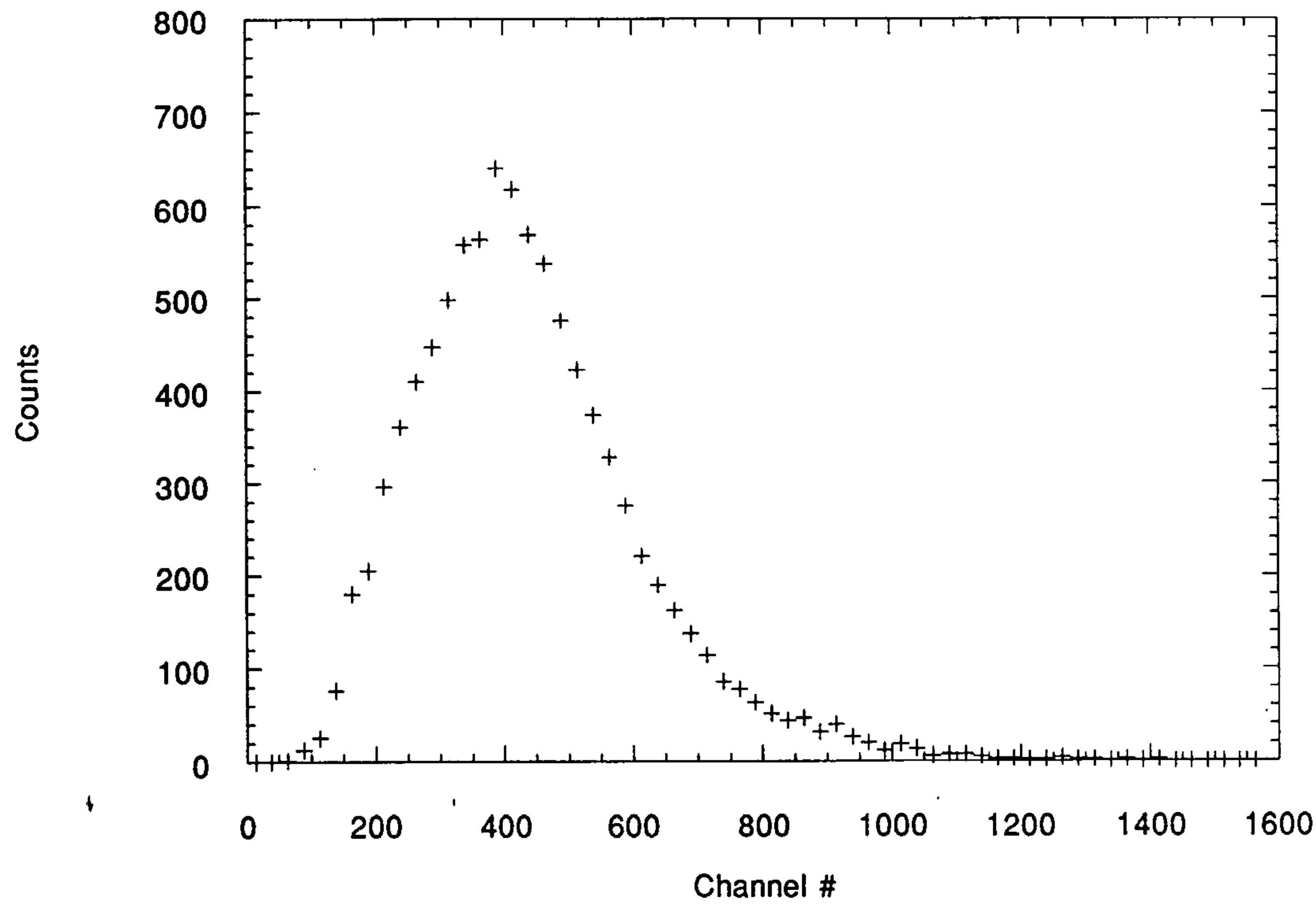
800
700
600
500
400
300
200
100
0
Counts
0
200
400
600
800
1000
1200
1400
1600
Channel #

Figure 2c

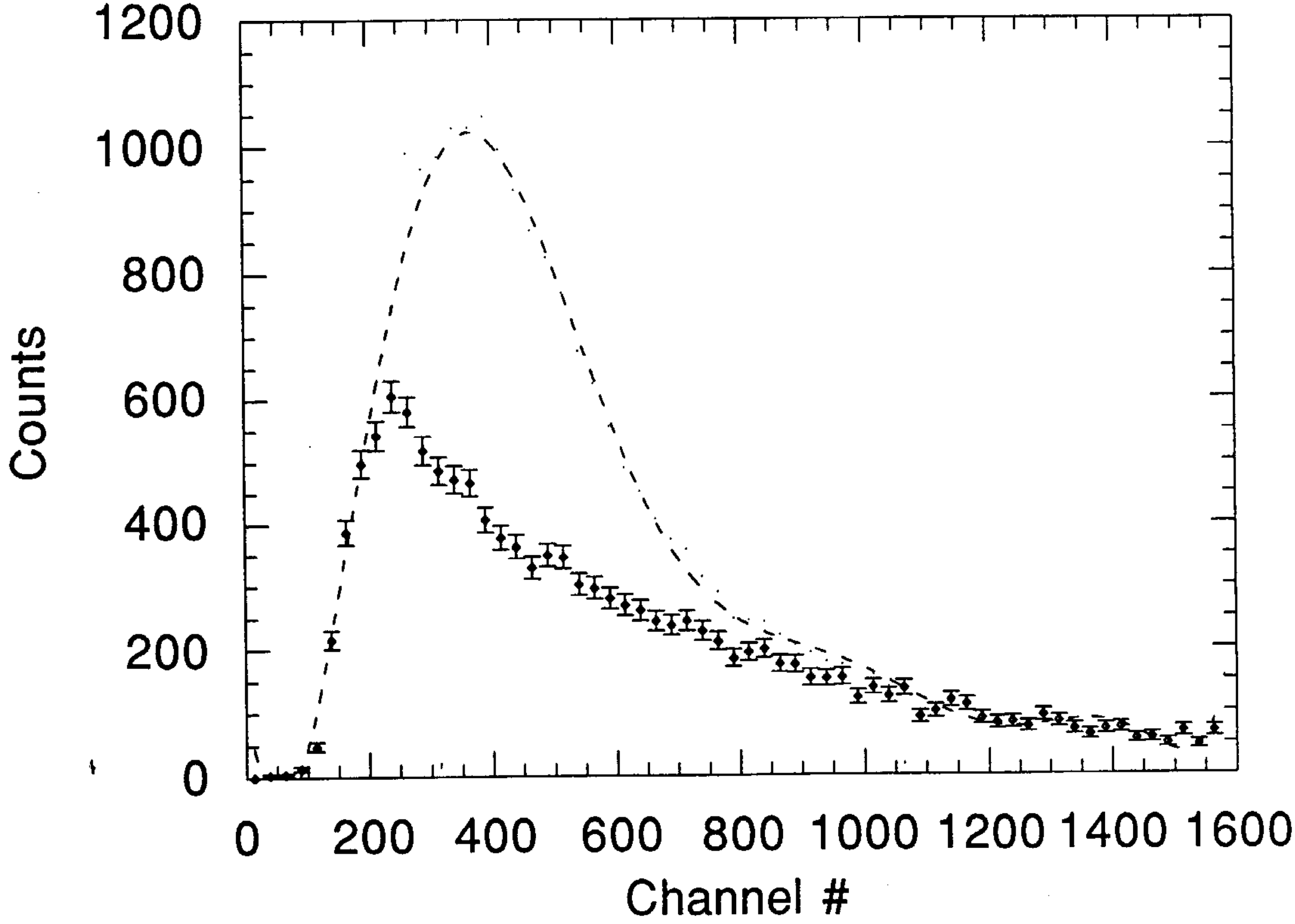
1200
1000
800
600
400
200
0
Counts
0
200
400
600
800
1000
1200
1400
1600
Channel #

Figure 3a

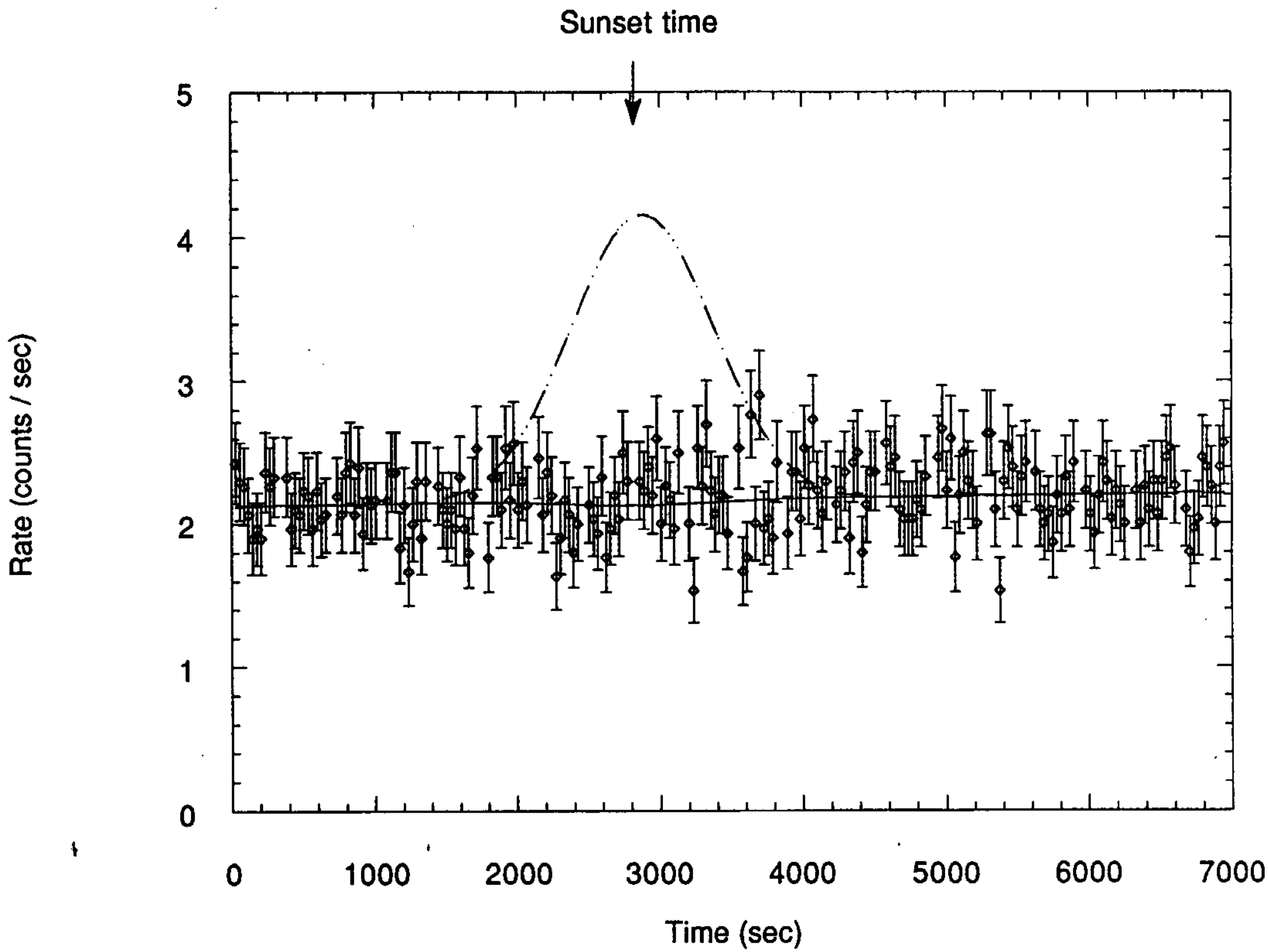
Sunset time
5
4
3
2
1
0
Rate (counts / sec)
0
1000
2000
3000
4000
5000
6000
7000
Time (sec)

Figure 3b

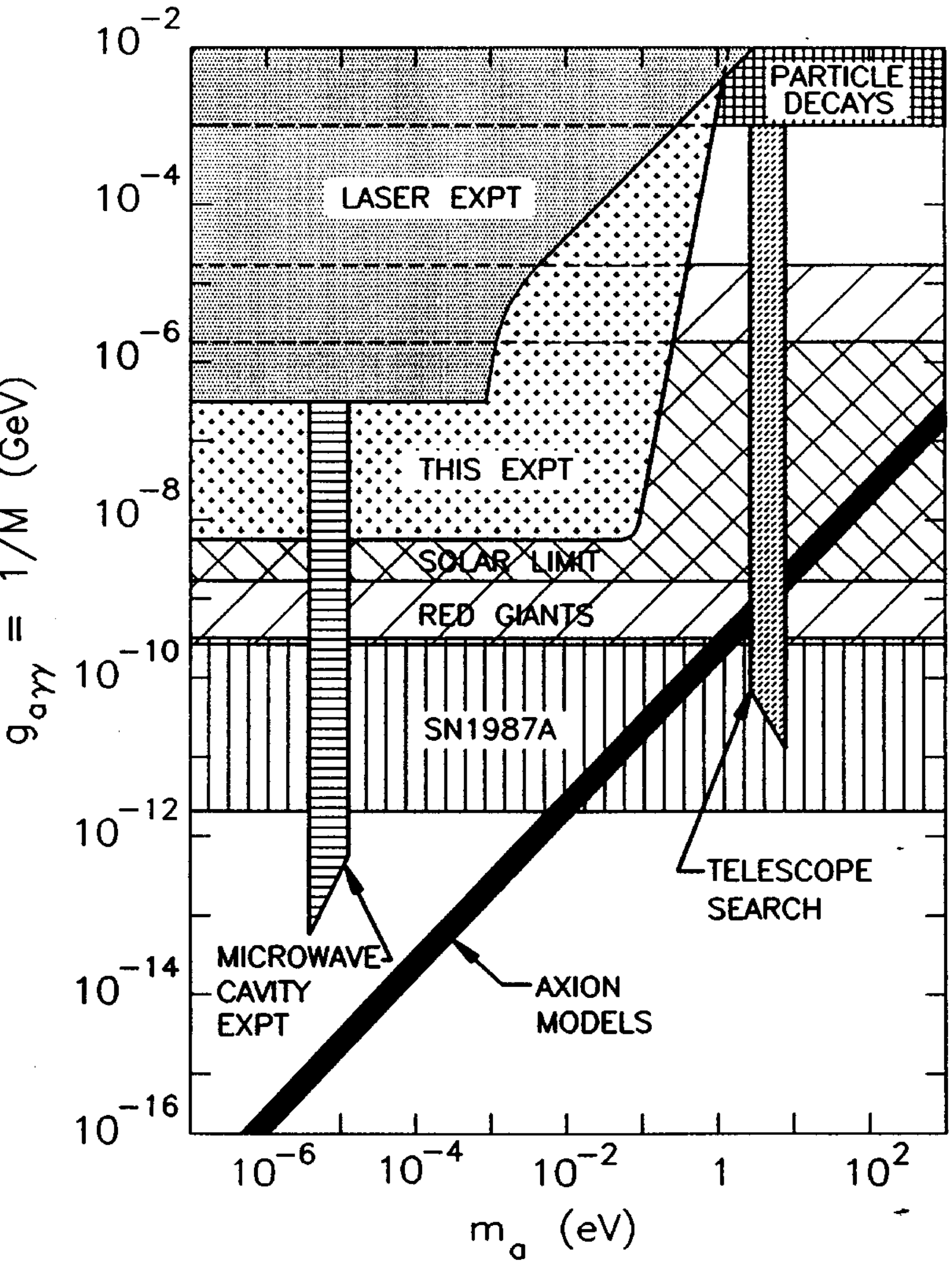
PARTICLE DECAYS
LASER EXPT
THIS EXPT
SOLAR LIMIT
RED GIANTS
SN1987A
MICROWAVE CAVITY EXPT
AXION MODELS
TELESCOPE SEARCH
$g_{a\gamma\gamma} = 1/M\ (GeV)^{-1}$
m_a (eV)
10^{-2}
10^{-4}
10^{-6}
10^{-8}
10^{-10}
10^{-12}
10^{-14}
10^{-16}
10^{-6}
10^{-4}
10^{-2}
1
10^{2}

Figure 4